Discontinuous-PWM Method for Multilevel N-Cell Cascaded H-Bridge Converters

Discontinuous-PWM Method for Multilevel N-cell Cascaded H-bridge Converters

Abraham Marquez, *Member, IEEE*, Vito Giuseppe Monopoli, *Senior Member, IEEE*, Anatolii Tcai *Member, IEEE*, Jose I. Leon, *Fellow, IEEE*, Giampaolo Buticchi, *Senior Member, IEEE*, Sergio Vazquez *Senior Member, IEEE*, Marco Liserre, *Fellow, IEEE*, Leopoldo Garcia Franquelo *Life Fellow, IEEE*

***Abstract*—The cascaded H-bridge converter (CHB) is a very suitable solution with inherent modularity for many applications such as flexible ac transmission systems and motor drives. In this paper, the discontinuous pulse-width-modulation (DPWM) by clamping some power cells is used in the CHB because it permits to reduce the switching losses in the power devices. However, this provokes a high harmonic distortion (base-bands and side-bands harmonics) in the CHB output voltage compared with the quality obtained avoiding to clamp cells, just applying the conventional phase-shifted PWM (PS-PWM) technique. This has been studied for the three-cell CHB topology but the extension for a N-cell CHB with several clamped cells is a challenge that is addressed in this work. A generalized CHB harmonic voltage analysis applying the DPWM method is presented considering multiple clamped cells. The harmonic distortion mitigation target can be decoupled into two objectives. The proposed method cleverly groups the cells (one clamped + one or two non-clamped cells) to mitigate the base-bands harmonic distortion. Simultaneously, a variable-angle PS-PWM technique is applied to the CHB in order to mitigate the side-bands harmonics content. Experimental results demonstrate the good performance of the proposed method.**

I. Introduction

Multilevel converters can be considered as a mature technology in the last decades. In fact, there are multiple industry applications where they are being successfully applied such as variable frequency drives, power transmission, motor drives and flexible ac transmission systems just to name a few [1]. Among the multilevel converters, the cascaded H-bridge (CHB) topology, that it is shown in Fig. 1 (single-phase topology), is one of the most popular ones [2]. CHB is formed by the serial connection of identical H-bridges (also called power cells) as shown in Fig. 1. Among its advantages, CHB is able to achieve high output voltages with very high quality. These facts are achieved by a CHB composed by a large number of cells [3]. In addition, CHB presents a natural fault-tolerant capability due to its inherent modularity which enables to CHB for sensible applications. This fact makes the CHB with large number of cells a perfect candidate for medium- and high-voltage applications such as silicon-based smart transformers, flexible ac transmissions systems, high-voltage dc transmission systems and motor drives [4]–[7]. As commercial examples, the nine-cell Sinamics Perfect Harmony GH180 and the eight-cell NC HVVF by Nancal can be found in the market [8], [9].

It is possible to use different methods to operate a CHB. These methods can be based on the generation of optimal pulses trends such as the pre-programmed PWM selective harmonic control methods or multi-carrier based modulation techniques [10]. Conventionally, the CHB is usually operated using the conventional phase-shifted pulse-width modulation (PS-PWM) technique. In this modulation method, each power cell is operated using the well-known unipolar PWM technique with carrier frequency f_c. The traditional PS-PWM implementation requires a phase displacement of the carrier signals between power cells equals to π divided by number of available cells in each phase (N) [11]. This concept is also illustrated in Fig. 1, where ϕ_j represents the phase displacement angle of the carrier signals of power cell j:

$$\phi_j = (j-1)\frac{\pi}{N} \qquad j = 1, 2, \ldots N \tag{1}$$

The application of the PS-PWM method to the CHB converter has many advantages such as an equal distribution of the power among the power cells leading to the equalization of the power losses and therefore, the aging equalization of the power devices [12]. In addition, the PS-PWM method generates an inherent multiplicative effect in the output voltage switching frequency. Applying the PS-PWM method, the CHB output voltage presents an effective switching frequency equal to $2Nf_c$ [11]. The operation of the CHB applying the PS-PWM method with f_c equal to 1 kHz is shown in Fig. 2 from 0 to 40 ms.

As it is well known, the harmonic spectrum can be split-off in three different parts, that are the fundamental, the base-bands and the side-bands components. To illustrate and clarify these concepts, an example of a typical harmonic spectrum of the output voltage of a power cell in the CHB applying a unipolar PWM is shown in Fig. 3. In the harmonic spectrum, the base-bands components are located at low frequency orders

Manuscript received Feb 2020; revised June 2020, accepted July, 2020. A. Marquez, J. I. Leon, S. Vazquez and L. Franquelo are with the University of Seville, Spain (e-mail: amarquez@ieee.org). V. G. Monopoli is with the Technical University of Bari, Italy (vitogiuseppe.monopoli@poliba.it). A. Tcai and M. Liserre are with the Christian-Albrechts Universitaet zu Kiel, Germany (ta@tf.uni-kiel.de, liserre@ieee.org). G. Buticchi is with the University of Nottingham Ningbo China, 199 Taikang East Road, 315100, China (phone: +86(0)574 88180000-8716 e-mail: buticchi@ieee.org).

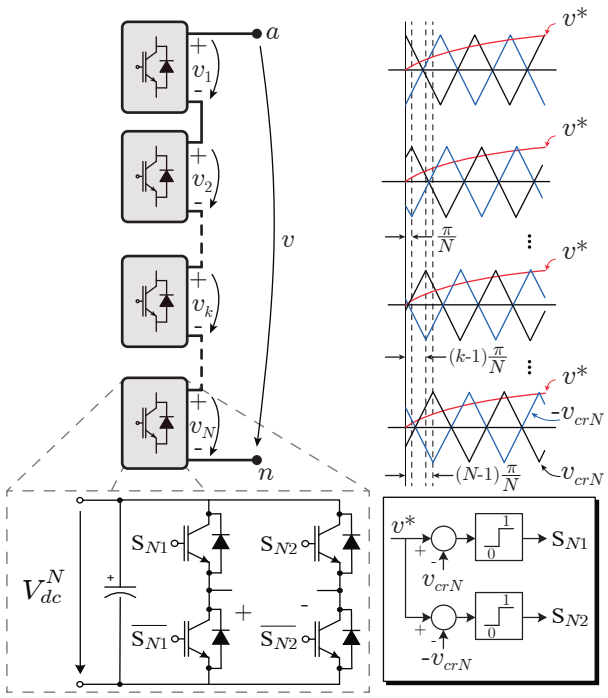

Fig. 1: Generalized multilevel cascaded H-bridge converter (CHB): Topology and conventional PS-PWM technique

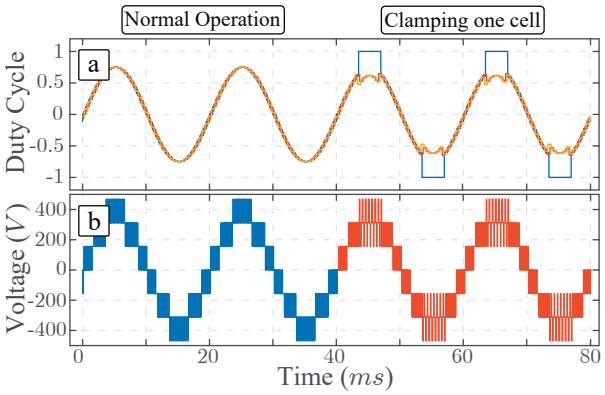

Fig. 2: CHB output voltage applying the conventional PS-PWM method with the same voltage reference per cell (0-40 ms) and forcing one clamping one cell (DPWM method) (40-80 ms)

and the side-bands components are created by the switching of the power converter. Keeping this in mind, the corresponding harmonic spectrum of a three-cell CHB converter is represented in Fig. 5a. It can be observed that the application of the PS-PWM method with CHB balanced operation (equal dc voltages and equal voltage references in the power cells) lead to the elimination of both the base-bands harmonics and the side-bands components up to the harmonic group $m = N$ that corresponds to frequency around $2Nf_c$.

It has to be noticed that in the current power electronics area, research and industry is focused on maximizing the multilevel converters efficiency by reducing the power losses [13]–[15] and also extending as much as possible the converter remaining useful lifetime (RUL) [16]–[18]. One option to

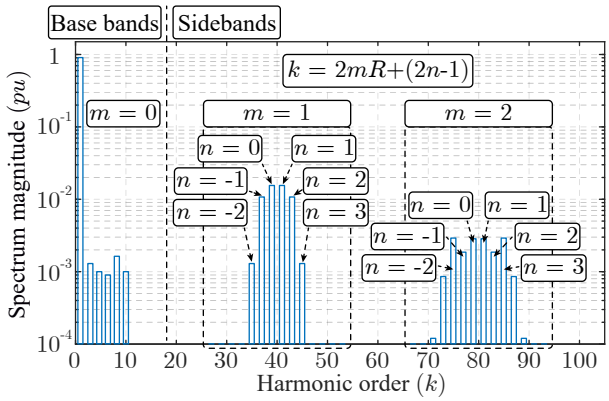

Fig. 3: Typical harmonic spectrum of a power cell output voltage in a CHB

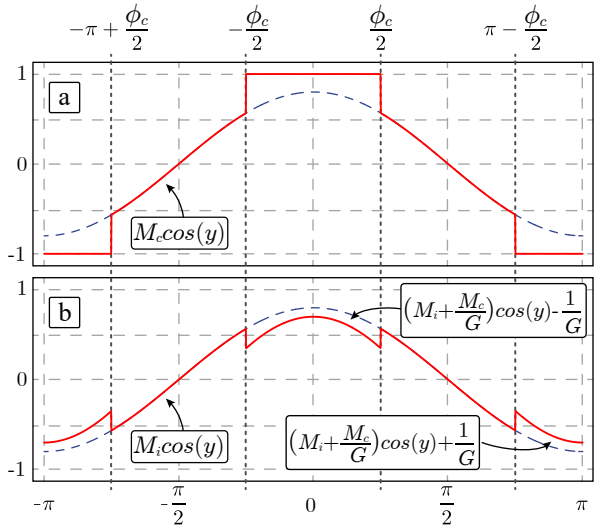

Fig. 4: Normalized reference voltage waveform to be generated by a) a clamped cell b) a non-clamped cell

minimize the power losses in the CHB is the application of a discontinuous PWM (DPWM) method where some power cells of the converter are clamped [19], [20]. For instance, the DPWM is a conventional modulation method considered by some thermal management control strategies (commonly called active thermal control (ATC) methods) [21], [22].

The DPWM method applied to the CHB is shown in Fig. 2 from 40 to 80 ms. During the clamping period, the clamped cells do not present switching losses increasing the converter efficiency. It is important to notice that, as shown in Fig. 2, the non-clamped cells have to compensate the extra voltage generated by the clamped cells. In this way, in the proposed method the cells can be organized in groups where one clamped cell is compensated by one or several non-clamped cells.

A detail of the DPWM method for the CHB considering the clamped and the non-clamped cells is represented in Fig. 4. The clamping instant of the cells is defined by the clamping angle ϕ_c that is determined accordingly with the switching losses reduction target. In a specific group of cells, M_i is

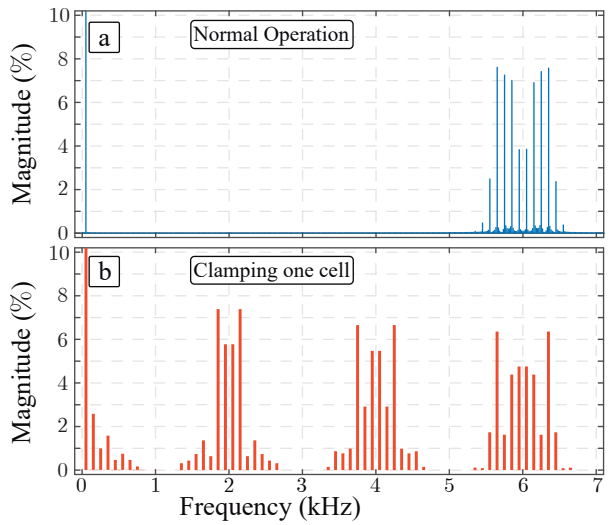

Fig. 5: CHB output voltage harmonic spectrum applying the conventional PS-PWM method a) with the same voltage reference per cell (0-40 ms) b) forcing one clamping one cell (DPWM method)

the modulation index of the non-clamped cell C_i, M_c is the modulation index of the clamped cell in the group and G is the number of non-clamped cells in the group (in this work for the sake of simplicity, G can be equal to 1 or 2).

The resulting CHB output voltage harmonic spectrum applying the DPWM method and the conventional PS-PWM technique for the non-clamped cells is represented in Fig.5c. As a drawback of the application of this modulation method, it is clear that a high harmonic distortion appears located at very low frequency, below the carrier frequency f_c (base-bands harmonics), and located above f_c (side-bands harmonics).

The harmonic degradation phenomenon of the CHB output voltage when the reference voltages of the cells are not identical (also including the possibility of presenting unequal dc voltages in the power cells) has been deeply studied. In particular, in [23] it is possible to find a performance comparison of different modulation techniques addressing these harmonic quality degradation issues. As an example of these techniques, in [24], [25] the use of heuristic algorithms to carry out the determination of the angle displacements to be applied to the PS-PWM method was proposed. On the other hand, a modified version of the PS-PWM method based on a mathematical description using the Fourier expansion series was presented in [26], [27]. This technique enables the possibility to operate the CHB converter with both different dc voltages and also different cell reference voltages. Improving the previous methods, in [28], [29] it is proposed the use of the DPWM method simultaneously working with the PS-PWM technique with variable phase displacement angles for a CHB converter taking into account unbalanced operational conditions (i.e. different modulation indices and dc voltages in the cells).

It is very important to highlight that the previous modulation methods dealing with the CHB output voltage harmonic degradation when the converter is operated with unbalanced conditions [23], [24], [26], [28], [29] are limited to CHB converters with three-cells per phase. This fact represents a hard limitation of these techniques. As it will be addressed in the work, the extension of this kind of methods is not a simple task.

The objective of this paper is to mitigate the CHB output voltage harmonic degradation by reducing both base-bands and side-bands harmonics when a DPWM method is applied for a N-cell CHB with several clamped cells. In particular, this work addresses a generalization of the modulation method presented in [28], [29] allowing to consider CHB converters with large number of cells (>3), permitting to have more than one clamped cell. Up to the authors' knowledge, it is the first time that this problem is solved. In this way, the proposed method opens the possibility to apply the DPWM method for this kind of converters, normally applied to medium- to high-power applications (where a high number of power cells are required to achieve such high nominal voltages).

II. Problem Statement

For the sake of simplicity to show how to deal with a N-cell CHB topology with more than one clamped cell, a four-cell CHB converter with two clamped cells (T_1, T_2) and two non-clamped cells (C_1, C_2) is considered. In this sense, two different DPWM operation schemes appear because the clamped cell T_x can be compensated with non-clamped cell C_y forming different groups of cells $[T_x, C_y]$ such as $[T_1, C_1]$-$[T_2, C_2]$ or $[T_1, C_2]$-$[T_2, C_1]$. As another example, considering a five-cell CHB converter with two clamped cells (T_1, T_2) and three non-clamped cells (C_1, C_2, C_3), the number of possible scenarios increases. For instance, it is possible to form cell groups such as $[T_1, C_1]$-$[T_2, C_2, C_3]$ or $[T_1, C_2]$-$[T_2, C_1, C_3]$ or other combinations. As it can be observed, the maximum number of possible combinations to be considered in a DPWM method for the CHB grows as the number of cells increases.

III. Generalized Harmonic Analysis of the CHB Output Voltage Considering Clamped and Non-Clamped Cells Using the PS-PWM Method

In order to determine the harmonic content of the CHB output voltage, each power cell output voltage is analyzed using the double Fourier series. As it is well known, the harmonic spectrum can be split-off in three different parts, that are the fundamental, the base-bands and the side-bands components. To illustrate and clarify these concepts, an example of a typical harmonic spectrum of the output voltage of a power cell in the CHB applying a unipolar PWM is shown in Fig. 3. In the harmonic spectrum, the base-bands components are located at low frequency orders and the side-bands components are created by the switching of the power converter and are located at multiples of $2f_c$ (in Fig. 3 the fundamental component is $f_0 = 50\ Hz$ and f_c is $1\ kHz$, therefore $R = f_c/f_0 = 20$). The indices m and n are used to identify the harmonic component of harmonic order $k = 2mR + (2n - 1)$.

A. Clamped Cell Output Voltage Description

Assuming the normalized reference voltage for a clamped cell shown in Fig. 4a, the different harmonic components can be calculated. In order to facilitate and simplify the obtained expressions, the factor $Z(x)$ is defined as

$$Z(x) = \frac{\sin(x\phi_c)}{x}. \tag{2}$$

The fundamental component of a clamped cell T_i applying a clamping angle ϕ_c is determined as

$$H_1^c = \frac{V_{dc}^c}{\pi}\Big[M_c(\pi - \phi_c - Z(1)) + 2Z(1/2)\Big] \tag{3}$$

where V_{dc}^c and M_c are respectively the dc voltage and the modulation index of the clamped cell.

On the other hand, the magnitude of each base-bands component of harmonic order $k = 2mR + (2n-1)$ in the output voltage of a clamped cell is obtained imposing $m = 0$ and $n > 0$ as

$$H_{bb}^c(n) = \frac{V_{dc}^c}{\pi}\left[2Z(a/2) - M_c\Big(Z(n) + Z(b)\Big)\right] \tag{4}$$

where $a = 2n-1$, $b = n-1$.

Finally, the magnitude of each particular harmonic component n of the harmonic group m in the side-bands frequencies can be calculated as:

$$H_{sb}^c(m,n) = A_1A_3(\pi - \phi_c - Z(a))J_a(A_2)\Big|_{\substack{if\rho=n\\ if\rho=1-n}} - \sum_{\substack{\rho=1\\ \rho\neq n, if n>0\\ \rho\neq 1-n, if n\leq 0}}^{\infty}\Big(-A_1A_4\big(Z(d)+Z(e)\big)J_{2\rho-1}(A_2)\Big) \tag{5}$$

where J_x is the Bessel function of the first kind of order x, and the auxiliary variables A_1, A_2, A_3 and A_4 are defined as

$$A_1 = \frac{2V_{dc}^c}{m\pi^2} \qquad A_2 = m\pi M_c$$
$$A_3 = \cos(c\pi) \qquad A_4 = \cos\Big((m+\rho-1)\pi\Big) \tag{6}$$

where $c = m+n-1$, $d = n+\rho-1$ and $e = n-\rho$.

B. Non-clamped Cell Output Voltage Description

Assuming that the cell T_i has been clamped, the normalized reference voltage of a non-clamped cell C_i that compensates it, is represented in Fig. 4b. The fundamental component of a non-clamped cell C_i that compensates the clamping of T_i can be obtained as

$$H_1^i = \frac{V_{dc}^i}{\pi}\left[M_i\pi + \frac{M_c}{G}\Big(\phi_c + Z(1)\Big) - \frac{2}{G}Z(1/2)\right] \tag{7}$$

Considering the base-bands components ($m = 0$, $n > 0$), each particular component can be described as:

$$H_{bb}^i(n) = \frac{V_{dc}^i}{\pi}\left[\frac{M_c}{G}\Big(Z(n) + Z(b)\Big) - \frac{2}{G}Z(a/2)\right] \tag{8}$$

Finally, for the side-bands components it is necessary to know if the clamped cell is compensated by one or two power cells (corresponding to G equal to 1 or 2) because the harmonic description is slightly different for both cases. For both cases and for each value of the indices m and n, the the amplitude of the side-bands can be calculated according to the expressions in Table I.

C. CHB Output Voltage Description

The output voltage of each cell can be described using the previous expressions as the sum of the fundamental component, the base-bands and the side-bands harmonics as

$$v_j(t) = H_1^j\cos(\omega_0 t) + \sum_{n=2}^{\infty} H_{bb}^j(n)\cos(a\omega_0 t) + \sum_{m=1}^{\infty}\sum_{n=-\infty}^{\infty} H_{sb}^j(m,n)\cos(2m\omega_c t + a\omega_0 t + 2m\phi_j) \tag{9}$$

where ω_0 is the pulsation of the modulating signal, ω_c is the pulsation of the carrier signal and ϕ_j is the phase displacement angle of the carriers of the cell j. From the previous expression, it can be noticed that the base-bands harmonics do not depend on ϕ_j. The values of the phase displacement angles of the carrier signals ϕ_j only affect to the side-bands harmonics.

Finally, the CHB output voltage can be calculated as the sum of each power cell voltage as:

$$v(t) = \sum_{j=1}^{N} v_j(t) \tag{10}$$

It is important to highlight that the addressed mathematical analysis of the harmonic content of the CHB output voltage is general and valid for any switching frequency f_c.

IV. CHB Output Voltage Optimization

The base-bands and side-bands harmonics of the output voltage of each cell are determined by the operation chosen by the DPWM method (the cells to be clamped and how the cell groups are formed) and the specific PS-PWM method implementation. Once the clamped cells are determined by the power losses management control method, the CHB output voltage harmonic spectrum can be improved if the cells are cleverly organized in groups, each one with one clamped cell and one or two non-clamped cells. The target of this grouping is to mitigate the base-bands harmonic content. On the other hand, the CHB output voltage harmonic performance can be further improved by applying a variable-angle PS-PWM technique [26]. In this modulation method, the phase displacement angles of the carrier signals are not fixed and vary in order to mitigate the side-bands harmonic distortion

TABLE I: Mathematical description of the side-bands harmonic components of a non-clamped cell

If the clamped cell is compensated by one cell (G=1) (11)

$$H^j_{sb}(m,n) = B_{1i}\Bigg[\Bigg[B_3\Big[\sin\Big((4m+|a|)\frac{\pi}{2}\Big)+\sin\Big(|a|\frac{\pi}{2}\Big)\Big]J_{|a|}(B_{2i}) - B_5\Big[\sin\Big((2m+|a|)\frac{\pi}{2}\Big)\Big]J_{|a|}(B_{4i})\Big] + \sum_{\substack{\rho=1\\ \rho\neq|a|}}^{\infty}\Delta\Bigg[\Big[\cos((a+\rho)\pi)\sin\Big((4m+\rho)\frac{\pi}{2}\Big)+\sin\Big(\rho\frac{\pi}{2}\Big)\Big]J_\rho(B_{2i}) - \Big[\sin\Big((2m+\rho)\frac{\pi}{2}\Big)(1+\cos\Big((a+\rho)\pi\Big)\Big]J_\rho(B_{4i})\Bigg]\Bigg]$$

If the clamped cell is compensated by one cell (G=2) (12)

$$H^j_{sb}(m,n) = B_{1i}\Bigg[B_6\Big[\cos(a\pi)\sin\Big(3m\frac{\pi}{2}\Big)+\sin\Big(m\frac{\pi}{2}\Big)\Big]J_0(B_{2i}) + \Bigg[B_3\Big[\sin\Big((3m+|a|)\frac{\pi}{2}\Big)+\sin\Big((m+|a|)\frac{\pi}{2}\Big)\Big]J_{|a|}(B_{2i}) - B_5\sin\Big((3m+|a|)\frac{\pi}{2}\Big)J_{|a|}(_{4i})\Big] + \sum_{\substack{\rho=1\\ \rho\neq|a|}}^{\infty}\Delta\Bigg[\Big[\cos((a+\rho)\pi)\sin\Big((3m+\rho)\frac{\pi}{2}\Big)+\sin\Big((m+\rho)\frac{\pi}{2}\Big)\Big]J_\rho(B_{2i}) - \Big[\sin\Big((2m+\rho)\frac{\pi}{2}\Big)(1+\cos\Big((a+\rho)\pi\Big)\Big]J_\rho(B_{4i})\Bigg]\Bigg]$$

$$B_{1i}=\frac{2V^i_{dc}}{m\pi^2}\quad B_{2i}=m\pi\left(M_i+\frac{M_c}{G}\right)\quad B_3=\frac{(Z(a)+\phi_c)}{2}\quad B_{4i}=m\pi M_i\quad B_5=Z(a)-\pi+\phi_c\quad B_6=\frac{Z(a)}{2}$$

$$\Delta = 0.5\Big(Z\Big(\frac{(a+\rho)}{2}\Big)+Z\Big(\frac{(a-\rho)}{2}\Big)\Big) \quad (13)$$

TABLE II: Example of operational conditions in a five-cell CHB where two cells are clamped in order to implement a DPWM method

Parameter	Values				
Cell number	1	2	3	4	5
V^i_{dc} $[V]$	90	100	90	85	90
Modulation index	0.87	0.70	0.75	0.92	0.85
ϕ_c $[^\circ]$	0	80	60	0	0
Role Name	C_1	T_1	T_2	C_2	C_3

of the CHB output voltage. Therefore, in this work, the application of both methods (cells grouping and variable-angle PS-PWM) are simultaneously considered in order to mitigate both the base-bands and the side-bands harmonic contents respectively. It is important to notice that, taking into account the mathematical expressions previously addressed, it is demonstrated that the targets of both methods are decoupled.

In order to look for an enhanced harmonic spectrum of the CHB output voltage, any cost function to look for a specific harmonic shaping can be used. As an example, the cost function can consider the weighted total harmonic distortion with respect to the total dc voltage (WTHD0). The cost function τ includes the WTHD0$_{bb}$ that is considered up to 10^{th} harmonic order and the WTHD$_{sb}$ that considers up to harmonic order with $m = 3$ and $n = 6$):

$$\tau = \mathbf{WTHD0_{bb}} + \mathbf{WTHD0_{sb}} \quad (14)$$

In order to illustrate the proposed idea, a five-cell CHB converter is considered with the operational conditions summarized in Table II. It has to be noticed that these conditions have been chosen in order to show that the proposed method can be applied with different values of the dc voltages and modulation indices. Usually, the CHB operates with the same dc voltages and modulation indices in all the cells but this can be seen as a particular case of the study presented in this work. In any case, the values of the dc voltages references, the modulation index of each cell and the cells to be clamped to implement the DPWM method will be determined by the CHB operation imposed by the control method. In the example shown in Table II, the DPWM method fixes that cells number 2 and 3 have to be clamped in order to reduce their switching losses saving some of their RUL. The five-cell CHB converter with two clamped cells has six different options to form groups in order to implement the DPWM strategy. These options are summarized in the first column in Table III and Table IV.

First of all, the DPWM method is applied to the five-cell CHB and the conventional PS-PWM technique is used to generate the final switching signals of the power cells. The obtained results are summarized in Table III, where it can be seen that the best cells combination is formed by the groups $[T_1, C_1]$-$[T_2, C_2, C_3]$ where the cost function τ is minimum

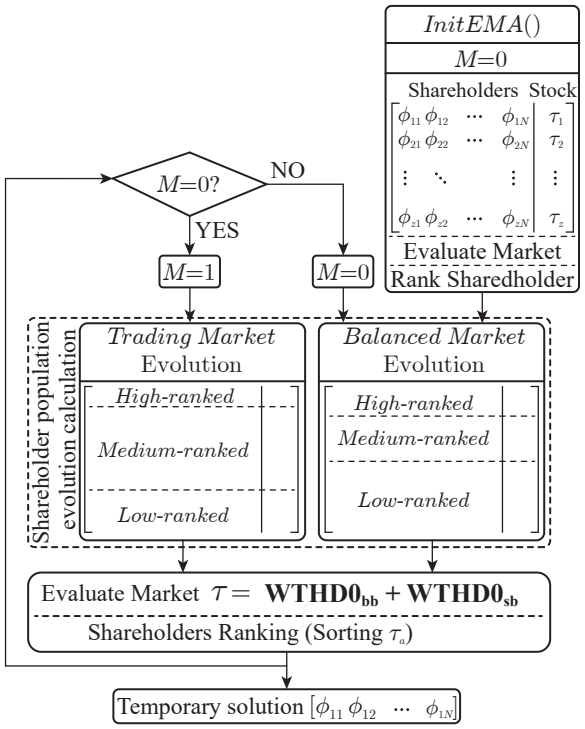

Fig. 6: Diagram of the EMA to find proper phase displacement angles in the variable-angle PS-PWM method to minimize the cost function τ

being equal to 0.3774.

In order to improve the results obtained in Table III, the variable-angle PS-PWM method can be applied to generate the switching signals of the CHB. In this work, due to the complexity of the cell voltage waveforms and the high number of possibilities to form the groups, a mathematical search algorithm has been used in order to find proper values of the phase displacement angles. As an example to implement this mathematical search, an exchange market algorithm (EMA) has been implemented as shown in Fig. 6 [30]. Anyway, it has to be highlighted that any other mathematical search algorithm can be also applied to look for the phase displacement angles of the variable-angle PS-PWM method [24], [25].

The obtained results applying the EMA to find the proper phase displacement angles of the variable-angle PS-PWM method to generate the switching signals when the DPWM technique is applied are summarized in Table IV. As commented previously, the variable-angle PS-PWM does not modify the base-bands components and only the side-bands components are modified. It can be observed that, applying the variable-angle PS-PWM method, the cells combination that achieves a minimum value of the cost function is that defined by $[T_1, C_3]$-$[T_2, C_1, C_2]$. In addition, the final value of the cost function τ is reduced achieving a final value equal to 0.2107.

In order to highlight the good performance of the proposed method, the corresponding harmonic spectrum considering the best cell combinations from Table III and Table IV are represented in Fig. 7. As expected, the base-bands components are the same using both approaches. However, the side-bands components are reduced applying the variable-angle PS-PWM

TABLE III: WTHD0 data and cost function value applying the DPWM method with the conventional PS-PWM technique

Operation scheme	WTHD0_{bb}	WTHD0_{sb}	τ
$[T_1, C_1, C_2]$-$[T_2, C_3]$	0.1117	0.2879	0.3996
$[T_1, C_1, C_3]$-$[T_2, C_2]$	0.1286	0.2760	0.4046
$[T_1, C_1]$-$[T_2, C_2, C_3]$	0.1086	0.2688	0.3774
$[T_1, C_2, C_3]$-$[T_2, C_1]$	0.1117	0.2839	0.3956
$[T_1, C_2]$-$[T_2, C_1, C_3]$	0.1341	0.2712	0.4053
$[T_1, C_3]$-$[T_2, C_1, C_2]$	0.1086	0.2900	0.3986

TABLE IV: WTHD0 data and cost function value applying the DPWM method with the variable-angle PS-PWM technique with phase-displacement angles determined by the EMA

Operation scheme	WTHD0_{bb}	WTHD0_{sb}	τ
$[T_1, C_1, C_2]$-$[T_2, C_3]$	0.1117	0.1081	0.2198
$[T_1, C_1, C_3]$-$[T_2, C_2]$	0.1286	0.1132	0.2418
$[T_1, C_1]$-$[T_2, C_2, C_3]$	0.1086	0.1027	0.2113
$[T_1, C_2, C_3]$-$[T_2, C_1]$	0.1117	0.1110	0.2227
$[T_1, C_2]$-$[T_2, C_1, C_3]$	0.1341	0.1289	0.2630
$[T_1, C_3]$-$[T_2, C_1, C_2]$	0.1086	0.1021	0.2107

method with the angles obtained by EMA. Considering the operational point described in Table II, the evolution of the phase displacement angles determined by the EMA (using the conventional phase displacement angles of the PS-PWM method as the initial solution in the mathematical search) as well as the cost function τ are shown in Fig. 8 up to EMA iteration number 100.

It is important to notice that adopting the proposed technique, the harmonic distortion mitigation does not occur during transients but it is guaranteed in steady state. However, the fundamental component is always achieved independently of the cells combination that is initially chosen and the phase displacement angles applied in the PS-PWM method. It is worth to mention that during the operation of the CHB in a particular operational condition, the current best solution (best cell combination with the proper phase displacement angles in the PS-PWM method) is applied. This solution is continuously updated always applying the up-to-date best power cell scheme and the best phase displacement angles. This can be observed in Fig. 8, where a transient in the operation point of the CHB converter is applied in EMA iteration number 100. In the operation point 2, the data described in Table II are modified and cells 1 and 4 become the clamped cells with clamping angles equal to $50°$ and $60°$, respectively. As it is shown in Fig. 8, starting from the final solution obtained in EMA iteration number 100, the method is iteratively looking for the best cell grouping and the best phase displacement angles of

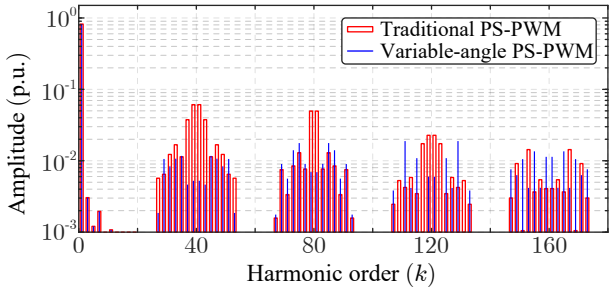

Fig. 7: CHB output voltage harmonic spectrum with the operations conditions summarized in Table II considering the best cells combination using the traditional PS-PWM method (blue) and the best cells combination applying the variable-angle PS-PWM method (red)

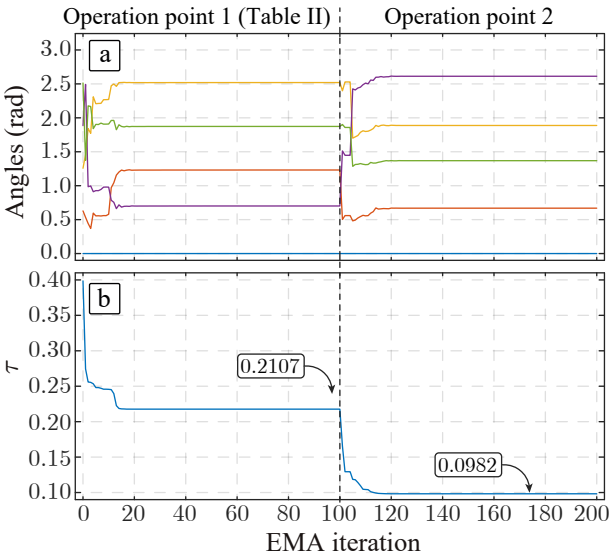

Fig. 8: Evolution of the EMA solutions looking for the phase displacement angles of the variable-angle PS-PWM method to minimize the cost function τ. A transient is forced in EMA iteration number 100.

the PS-PWM method to mitigate both base-bands and side-bands harmonics. After a few EMA iterations this mitigation is achieved as can be observed by the reduction of the cost function τ.

It is clear that the number of cell combinations to be considered is increasing with the number of power cells in the CHB. It can be noticed that, in order to determine the most proper cell combination, only the $WTHD0_{bb}$ has to be evaluated what reduces the computational cost (avoiding to initially determine $WTHD0_{sb}$). The $WTHD0_{bb}$ only needs to be calculated up to 10^{th} harmonic order and the corresponding computational cost is not excessive. Once the cells combination with minimum value of $WTHD0_{bb}$ is found, the EMA can be executed in order to determine the best phase displacement angles to be implemented in the PS-PWM method to reduce the $WHTD0_{sb}$. In this way, the computational cost of the method with large number of cells can be considered affordable. The computational capability of

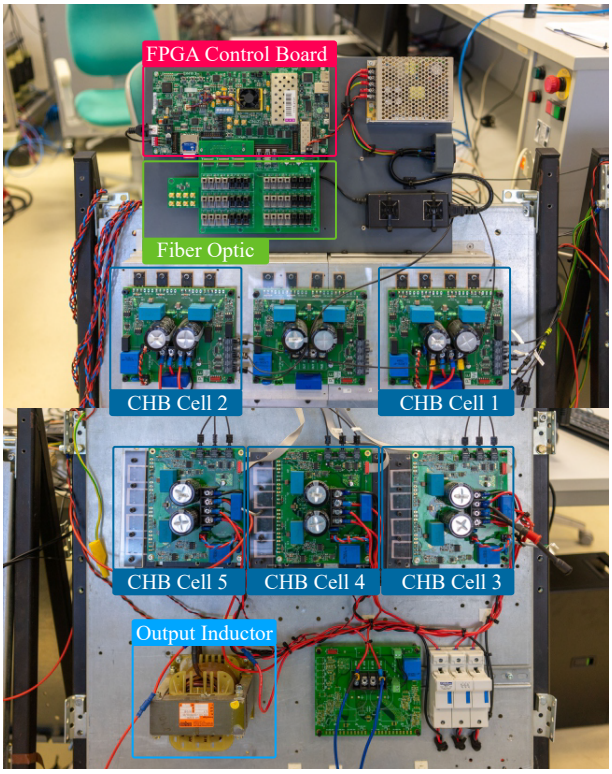

Fig. 9: Five-cell CHB down scaled laboratory prototype

the controller systems has experienced a huge growth in the last decades. There are multiple control platforms available in the manufacturer portfolio such as personal computers, server-based solutions, multi-core low-cost microcontrollers, FPGA, System of Chip (SoC) and cloud-based solutions. Currently they overcome the computational requirements with a very competitive price.

V. Experimental Results

In order to test the good performance of the proposed DPWM method with more than one clamped cell, the prototype shown in Fig. 9 has been used. This test rig is composed by five-cell CHB feeding a linear load. Each power cell is composed by four IXYB82N120C3H1 from IXYS and the whole power converter is handled by the Xilinx ZYNQ7000 zc706 FPGA [31], [32]. Additionally, the most important elements and parameters in the prototype are listed in Table V.

It has to be noticed that as the number of cells grows, the number of possible combinations to be analyzed and the number of phase-displacement angles to be determined by the EMA also grow. In this implementation done in the laboratory setup, the EMA iteration execution time is 1.1 millisecond. This could represent a limitation in the real-time implementation of the method (doing it offline and storing the results in look-up tables is always another feasible option). However, the computation capability of the modern control platforms is growing exponentially making huge advances in this area. Therefore, this computational burden limitation is a challenging barrier but it will be overcome in the near future by the next generations of control platforms.

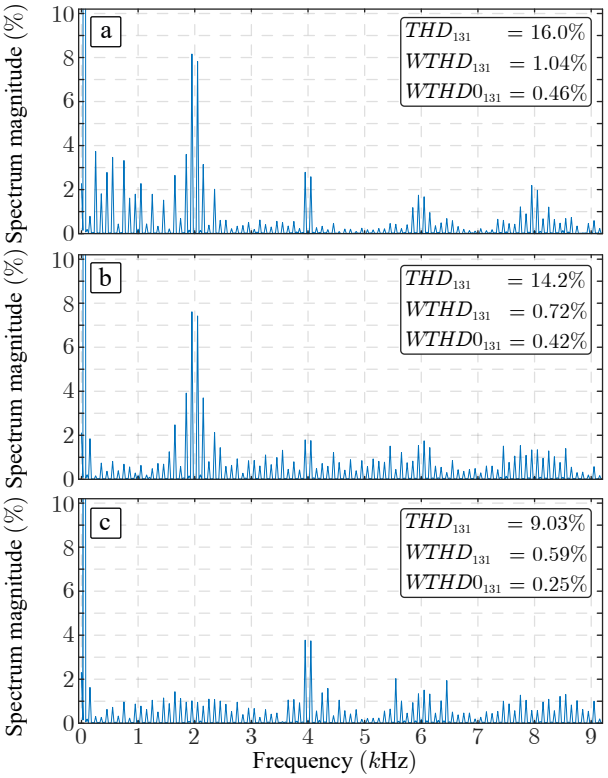

Fig. 10: CHB output voltage harmonic spectrum. a) $[T_1, C_2]$-$[T_2, C_1, C_3]$ cell combination with the traditional PS-PWM angles (row 5, Table III). b) $[T_1, C_3]$-$[T_2, C_1, C_2]$ cell combination with the traditional PS-PWM angles (row 6, Table III). c) $[T_1, C_3]$-$[T_2, C_1, C_2]$ cell combination with the variable-angle PS-PWM method using the phase-displacement angles solution set provided by EMA (row 6, Table IV).

The CHB converter has been operated with the conditions summarized in Table II. As a first test, in Fig. 10a the CHB output voltage considering the $[T_1, C_2]$-$[T_2, C_1, C_3]$ and the conventional PS-PWM angle set is shown. As it is expected, a non-negligible low-order harmonic distortion as well as a large harmonic distortion at twice the carrier frequency appear. The THD, WTHD and WTHD0 values considering up to 131^{st} harmonic order are considered. This harmonic order is the maximum component included in the cost function τ because $m{\leq}6$, $m{\leq}6$ and R=20 and $k = 2mR + (2n - 1)$.

As mentioned previously, the base-bands components depend on the cells combination whereas the side-bands components depend on the phase-displacement angles set. In this way, a second experiment has been performed considering the $[T_1, C_3]$-$[T_2, C_1, C_2]$ cells combination applying also the traditional PS-PWM method. It leads to improve the low-order harmonic content (base-bands components) which is clearly shown in Fig. 10b.

TABLE V: CHB parameters setup and passive elements considered for the experiment.

Parameter	Value
Number of cells in the CHB	5
Cell switching frequency f_c (kHz)	1
Cell DC Capacitance (mF)	2.2
Load Inductance (mH)	0.3
Load Resistance (Ω)	25

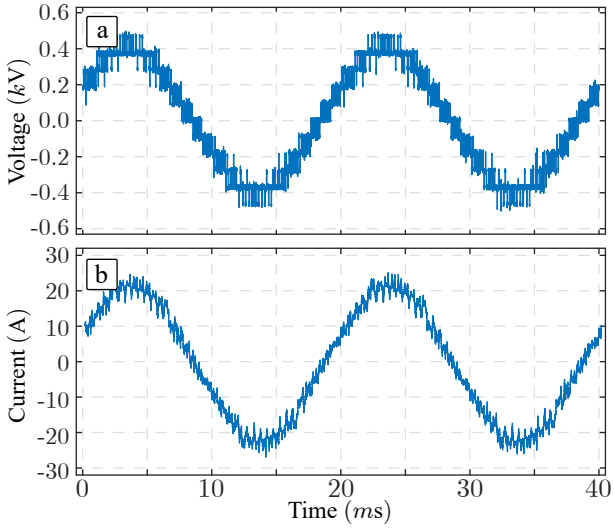

Fig. 11: CHB converter operation under $[T_1, C_3]$-$[T_2, C_1, C_2]$ power cell combination and the best angle solution set provided by EMA. a) Voltage. b) Current

Finally, the CHB converter has been operated considering the previous cell combination ($[T_1, C_3]$-$[T_2, C_1, C_2]$) but applying the variable-angle PS-PWM method with the angle solution set provided by EMA. In this case, the phase-displacement angles are $[0, 0.615, 1.918, 2.459, 1.201]$ radians for each power cell, respectively. The corresponding CHB output voltage and current are represented in Fig. 11. In these waveforms, some spikes are unavoidably created by the unbalanced operation of the CHB addressed in Table II. From this data, as it is shown in Fig. 10c, the side-bands components are reduced. The harmonic content located at $2f_c$ has suffered a significant reduction while the superior harmonics remain in acceptable values. Meanwhile, as expected, the base-bands components are not affected by the new phase-displacement angles.

VI. Conclusions

This paper is focused on the operation of CHB converters with any number of cells where some power cells are clamped. This is usual for instance in DPWM methods where the power cells RUL is managed by selecting the cells to be clamped in order to reduce their switching losses. However, these methods presents an important drawback in the output voltage harmonic spectrum because of the provoked undesirable distortion (both base-bands and side-bands). This paper deals with this phenomenon. The proposed method is based on the selection of the proper power-cell combination in a N-cell CHB in order to control the base-bands harmonics. Additionally, to control the side-bands harmonic components, the phase-displacement

angles of the carrier signals present in the PS-PWM method are also modified. Applying the proposed strategy, the DPWM method can be applied to the CHB with large number of power cells without reducing the output voltage quality performance.

It is important to highlight that the proposed method does not affect the converter loss. The power loss are related to the power cells clamping itself. If a DPWM method is implemented avoiding the use of grouping power cells and using the traditional PS-PWM method, the power losses compared with applying the proposed method are not modified. The objective of the proposed method is not related to reduce the loss but it is focused on improving the harmonic distortion of the CHB output voltage keeping the power losses unaffected.

REFERENCES

[1] M. Malinowski, K. Gopakumar, J. Rodriguez, and M. A. Perez, "A survey on cascaded multilevel inverters," *IEEE Transactions on Industrial Electronics*, vol. 57, no. 7, pp. 2197–2206, July 2010.

[2] W. Mcmurray, "Fast response stepped-wave switching power converter circuit," May 25 1971, uS Patent 3,581,212. [Online]. Available: https://www.google.com/patents/US3581212

[3] J. I. Leon, S. Vazquez, and L. G. Franquelo, "Multilevel converters: Control and modulation techniques for their operation and industrial applications," *Proceedings of the IEEE*, vol. 105, no. 11, pp. 2066–2081, Nov 2017.

[4] M. Liserre, G. Buticchi, M. Andresen, G. D. Carne, L. F. Costa, and Z. X. Zou, "The smart transformer: Impact on the electric grid and technology challenges," *IEEE Industrial Electronics Magazine*, vol. 10, no. 2, pp. 46–58, June 2016.

[5] L. F. Costa, G. D. Carne, G. Buticchi, and M. Liserre, "The smart transformer: A solid-state transformer tailored to provide ancillary services to the distribution grid," *IEEE Power Electronics Magazine*, vol. 4, no. 2, pp. 56–67, June 2017.

[6] F. Z. Peng, Y. Liu, S. Yang, S. Zhang, D. Gunasekaran, and U. Karki, "Transformer-less unified power-flow controller using the cascade multilevel inverter," *IEEE Transactions on Power Electronics*, vol. 31, no. 8, pp. 5461–5472, Aug 2016.

[7] Y. H. Liu, J. Arrillaga, and N. R. Watson, "Cascaded h-bridge voltage reinjection - part i: A new concept in multilevel voltage-source conversion," *IEEE Transactions on Power Delivery*, vol. 23, no. 2, pp. 1175–1182, April 2008.

[8] Siemens, "Sinamics perfect harmony gh180." [Online]. Available: https://new.siemens.com/global/en/products/drives/sinamics/medium-voltage-converters/sinamics-perfect-harmony-gh180.html

[9] Nancal, "Nancal nc hvvf converter." [Online]. Available: http://marstech.com.sg/wp-content/uploads/2017/09/Medium-Voltage-Drive.pdf

[10] J. I. Leon, S. Kouro, L. G. Franquelo, J. Rodriguez, and B. Wu, "The essential role and the continuous evolution of modulation techniques for voltage-source inverters in the past, present, and future power electronics," *IEEE Transactions on Industrial Electronics*, vol. 63, no. 5, pp. 2688–2701, May 2016.

[11] D. G. Holmes and T. A. Lipo. Wiley-IEEE Press, 2003, pp. 744–. [Online]. Available: http://ieeexplore.ieee.org/xpl/articleDetails.jsp?arnumber=5311953

[12] B. Wu and M. Narimani, *Cascaded H-Bridge Multilevel Inverters*. Wiley-IEEE Press, 2017, pp. 480–. [Online]. Available: http://ieeexplore.ieee.org/xpl/articleDetails.jsp?arnumber=7827420

[13] S. Rohner, S. Bernet, M. Hiller, and R. Sommer, "Modulation, losses, and semiconductor requirements of modular multilevel converters," *IEEE Transactions on Industrial Electronics*, vol. 57, no. 8, pp. 2633–2642, 2010.

[14] R. Picas, J. Zaragoza, J. Pou, S. Ceballos, G. Konstantinou, and G. J. Capella, "Study and comparison of discontinuous modulation for modular multilevel converters in motor drive applications," *IEEE Transactions on Industrial Electronics*, vol. 66, no. 3, pp. 2376–2386, 2019.

[15] N. Nguyen, B. Nguyen, and H. Lee, "An optimized discontinuous pwm method to minimize switching loss for multilevel inverters," *IEEE Transactions on Industrial Electronics*, vol. 58, no. 9, pp. 3958–3966, 2011.

[16] H. Lu, T. Tilford, C. Bailey, and D. R. Newcombe, "Lifetime prediction for power electronics module substrate mount-down solder interconnect," in *2007 International Symposium on High Density packaging and Microsystem Integration*, June 2007, pp. 1–10.

[17] I. F. Kovacevic, U. Drofenik, and J. W. Kolar, "New physical model for lifetime estimation of power modules," in *The 2010 International Power Electronics Conference - ECCE ASIA -*, June 2010, pp. 2106–2114.

[18] H. Salimian and H. Iman-Eini, "Fault-tolerant operation of three-phase cascaded h-bridge converters using an auxiliary module," *IEEE Transactions on Industrial Electronics*, vol. 64, no. 2, pp. 1018–1027, Feb 2017.

[19] C. Cecati, A. Dell'Aquila, A. Lecci, M. Liserre, and V. G. Monopoli, "A discontinuous carrier-based multilevel modulation for multilevel converters," in *30th Annual Conference of IEEE Industrial Electronics Society, 2004. IECON 2004*, vol. 1, 2004, pp. 280–285 Vol. 1.

[20] J. Hu, J. Lin, and H. Chen, "A discontinuous space vector pwm algorithm in abc reference frame for multilevel three-phase cascaded h-bridge voltage source inverters," *IEEE Transactions on Industrial Electronics*, vol. 64, no. 11, pp. 8406–8414, 2017.

[21] Y. Ko, M. Andresen, G. Buticchi, and M. Liserre, "Thermally compensated discontinuous modulation strategy for cascaded h-bridge converters," *IEEE Transactions on Power Electronics*, vol. 33, no. 3, pp. 2704–2713, March 2018.

[22] M. Liserre, G. Buticchi, J. I. Leon, A. Marquez, V. Raveendran, Y. Ko, M. Andresen, V. G. Monopoli, and L. G. Franquelo, "Power routing: a new paradigm for maintenance scheduling," *IEEE Industrial Electronics Magazine*, vol. 14, 2020.

[23] V. G. Monopoli, Y. Ko, G. Buticchi, and M. Liserre, "Performance comparison of variable-angle phase-shifting carrier pwm techniques," *IEEE Transactions on Industrial Electronics*, vol. 65, no. 7, pp. 5272–5281, July 2018.

[24] X. Cai, Z. Wu, Q. Li, and S. Wang, "Phase-shifted carrier pulse width modulation based on particle swarm optimization for cascaded h-bridge multilevel inverters with unequal dc voltages," 2015.

[25] A. Marquez Alcaide, J. I. Leon, V. G. Monopoli, S. Vazquez, M. Liserre, and L. G. Franquelo, "Generalized harmonic control for chb converters with unbalanced cells operation," *IEEE Transactions on Industrial Electronics*, pp. 1–1, 2019.

[26] A. Marquez, J. I. Leon, S. Vazquez, R. Portillo, L. G. Franquelo, E. Freire, and S. Kouro, "Variable-angle phase-shifted pwm for multilevel three-cell cascaded h-bridge converters," *IEEE Transactions on Industrial Electronics*, vol. 64, no. 5, pp. 3619–3628, May 2017.

[27] A. Marquez, J. I. Leon, R. Portillo, J. Yin, W. Luo, S. Vazquez, S. Kouro, and L. G. Franquelo, "Variable-angle ps-pwm technique for multilevel cascaded h-bridge converters with large number of power cells," *IEEE Transactions on Industrial Electronics*, vol. 99, 2020.

[28] V. G. Monopoli, A. Marquez, J. I. Leon, Y. Ko, G. Buticchi, and M. Liserre, "Improved harmonic performance of cascaded h-bridge converters with thermal control," *IEEE Transactions on Industrial Electronics*, vol. 66, no. 7, pp. 4982–4991, July 2019.

[29] A. Marquez, V. G. Monopoli, J. I. Leon, Y. Ko, G. Buticchi, S. Vazquez, M. Liserre, and L. G. Franquelo, "Sampling-time harmonic control for cascaded h-bridge converters with thermal control," *IEEE Transactions on Industrial Electronics*, vol. 67, no. 4, pp. 2776–2785, April 2020.

[30] N. Ghorbani and E. Babaei, "Exchange market algorithm," *Applied Soft Computing*, vol. 19, pp. 177 – 187, 2014. [Online]. Available: http://www.sciencedirect.com/science/article/pii/S156849461400074X

[31] IXYS, "xyb82n120c3h1 datasheet." [Online]. Available: https://www.ixys.com/

[32] Xilinx, "Zynq7000 zc702 fpga." [Online]. Available: https://www.xilinx.com/

Abraham Marquez (S'14, M'16) was born in Huelva, Spain, in 1985. He received his B.S. and M.S. degrees in telecommunications engineering in 2014 and 2016 from the Universidad de Sevilla (US), Spain, where he is currently working toward the PhD degree in electronic engineering.

His main research interest are modulation techniques, multilevel converters, power conversion for renewable energy sources and model-based predictive control of power converters and drives. Mr. Marquez was recipient as coauthor of the 2015 Best Paper Award of the IEEE Industrial Electronics Magazine.

Vito Giuseppe Monopoli (S'98-M'05-SM'18) received the M.Sc. and Ph.D. degrees in electrical engineering from the Bari Polytechnic, in 2000 and 2004, respectively. He is currently an Assistant Professor Bari Polytechnic, Bari, Italy. His research activity concerns multilevel converters and the analysis of harmonic distortion produced by power converters and electrical drives. He is particularly interested in innovative control techniques for power converters. He is member of the IEEE Industry Applications Society, IEEE Industrial Electronics Society and IEEE Power Electronics Society.

Anatolii Tcai (S'17) received the B.Sc. and M.Sc. in electrical and computer engineering from Tomsk State University of Control Systems and Radioelectronics (TUSUR), Tomsk, Russia and Ajou University, Suwon, Republic of Korea, in 2013 and 2018, respectively. He is currently employed as an industrial Ph.D. in Digital Twin Concepts for High Power Converters at Huawei Technologies R&D, Nuremberg, Germany and Christian-Albrechts University of Kiel, Kiel, Germany His current research interests include grid-connected systems, multilevel converters, discontinuous modulation and reliability in power electronics.

Jose I. Leon (S'04-M'07-SM'14-F'17) was born in Cadiz, Spain. He received the B.S., M.S., and PhD degrees in telecommunications engineering from Universidad de Sevilla (US), Seville, Spain, in 1999, 2001, and 2006, respectively. Currently, he is an Associate Professor with the Department of Electronic Engineering, US. Since 2019 he is also Chair Professor at the Department of Control Science and Engineering in Harbin Institute of Technology (China).

His research interests include modulation and control of power converters for high-power applications and renewable energy systems. Dr. Leon was a co-recipient of the 2008 Best Paper Award of IEEE Industrial Electronics Magazine, the 2012 Best Paper Award of the IEEE Transactions on Industrial Electronics, and the 2015 Best Paper Award of IEEE Industrial Electronics Magazine. He was the recipient of the 2014 IEEE J. David Irwin Industrial Electronics Society Early Career Award, the 2017 IEEE Bimal K. Bose Energy Systems Award and the 2017 Manuel Losada Villasante Award for excellence in research and innovation. In 2017 he was elevated to the IEEE fellow grade with the following citation "for contributions to high-power electronic converters".

Giampaolo Buticchi (S'10-M'13-SM'17) received the Master degree in Electronic Engineering in 2009 and the Ph.D degree in Information Technologies in 2013 from the University of Parma, Italy. In 2012 he was visiting researcher at The University of Nottingham, UK. Between 2014 and 2017, he was a post-doctoral researcher and Von Humboldt Post-doctoral Fellow at the University of Kiel, Germany. He is now Professor in Electrical Engineering at The University of Nottingham Ningbo China and the Head of Power Electronics of the Nottingham Electrification Center. His research focuses on power electronics for renewable energy systems, smart transformer fed micro-grids and dc grids for the More Electric Aircraft. He is author/co-author of more than 200 scientific papers and an Associate Editor of the IEEE Transactions on Industrial Electronics and of the IEEE Transactions on Transportation Electrification. He is the Chair of the IEEE Industrial Electronics Society Technical Committee on Renewable Energy Systems.

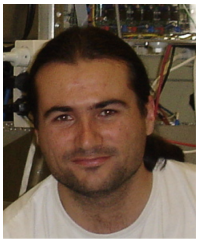

Sergio Vazquez (S'04-M'08-SM'14) was born in Seville, Spain, in 1974. He received the M.S. and PhD degrees in industrial engineering from the University of Seville (US) in 2006, and 2010, respectively. Since 2002, he is with the Power Electronics Group working in RD projects. He is an Associate Professor with the Department of Electronic Engineering, US. His research interests include power electronics systems, modeling, modulation and control of power electronics converters applied to renewable energy technologies. Dr. Vazquez was recipient as coauthor of the 2012 Best Paper Award of the IEEE Transactions on Industrial Electronics and 2015 Best Paper Award of the IEEE Industrial Electronics Magazine. He is involved in the Energy Storage Technical Committee of the IEEE industrial electronics society and is currently serving as an Associate Editor of the IEEE Transactions on Industrial Electronics.

Marco Liserre (S'00-M'02-SM'07-F'13) received the M.S. and PhD degree in Electrical Engineering from the Bari Polytechnic, respectively in 1998 and 2002. He has been Associate Professor at Bari Polytechnic and from 2012 Professor in reliable power electronics at Aalborg University (Denmark). From 2013 he is Full Professor and he holds the Chair of Power Electronics at Kiel University (Germany), where he leads a team of more than 20 researchers with an annual budget of 2 Mill. Euro and cooperation with 20 companies. He has published over 350 technical papers (more than 110 of them in international peer-reviewed journals) and a book. These works have received more than 25000 citations. Marco Liserre is listed in ISI Thomson report "The world's most influential scientific minds" from 2014.

He has been awarded with an ERC Consolidator Grant for the project "The Highly Efficient And Reliable smart Transformer (HEART), a new Heart for the Electric Distribution System" and with the ERC Proof of Concept Grant U-HEART.

He is member of IAS, PELS, PES and IES. He has been serving all these societies in different capacities. He has received the IES 2009 Early Career Award, the IES 2011 Anthony J. Hornfeck Service Award, the 2014 Dr. Bimal Bose Energy Systems Award, the 2011 Industrial Electronics Magazine best paper award the Third Prize paper award by the Industrial Power Converter Committee at ECCE 2012, 2012, the 2017 IEEE PELS Sustainable Energy Systems Technical Achievement Award and the 2018 IEEE IES Mittelmann Achievement Award which is the highest award of the IEEE-IES.

Leopoldo G. Franquelo (M'84-SM'96-F'05-LF'20) was born in Málaga, Spain. He received the M.Sc. and Ph.D. degrees in electrical engineering from the Universidad de Sevilla, Seville, Spain, in 1977 and 1980, respectively. He was associate professor from 1982-86 at the Electronics Engineering Department in Sevilla University and currently is professor at the Electronics Engineering Department in Sevilla University since 1986 and a 1000 Talent Professor at the Department of Control Science and Engineering in Harbin Institute of Technology since 2016. His current research interests include modulation techniques for multilevel inverters and application to power electronic systems for renewable energy systems. He has participated in more than 100 Industrial and R&D projects and has published more than 300 papers, 76 of them in IEEE Journals. Dr. Franquelo is an IEEE Fellow since 2005 and an IEEE Industrial Electronics Society (IES) Distinguished Lecturer since 2006. In the IEEE TRANSACTIONS ON INDUSTRIAL ELECTRONICS, he became an Associate Editor in 2007, Co-Editor-in-Chief in 2014, and the Editor-in-Chief since 2016. He was a Member-at-Large of the IES AdCom (2002-2003), Vice President for Conferences (2004-2007), and President Elect of the IES (2008-2009). He was the President of the IES (2010-2011) and is an IES AdCom Life member. In 2009 and 2013, he received the prestigious Andalusian Research Award and FAMA Award recognizing the excellence of his research career. He has received a number of Best Paper Awards from IEEE journals. In 2012 and 2015, he was the recipient of the Eugene Mittelmann Outstanding Research Achievement Award and the Antohny J. Hornfeck Service Award from IEEE-IES, respectively.